Preparation of adsorption material through calcining waste diatomite for treatment of dye water

He Zhang, Baoli Shi*, Lina Jia

College of Science, Northeast Forestry University, Harbin, 150040, China, Tel. +86-451-82192327,
email: 18366881589@163.com (H. Zhang), shi_baoli_nefu@163.com (B. Shi), lina_Jia@126.com (L. Jia)

ABSTRACT

In the production process of blueberry juice, diatomite is generally selected as filter. To utilize waste diatomite, high-temperature calcination was applied to treat waste diatomite at 500, 550, 600, 650, and 700°C. Adsorption capability of calcined products for adsorbing five dyes of crystal violet, methylene blue, rhodamine B, eosin Y, and methyl orange was explored. It was found that when calcination temperature was above 600°C, organic matter in waste diatomite would be decomposed thoroughly. No obvious change was observed in silica phase and the structure of diatom shell was not destroyed. Average particle diameter of calcined products was between 40 and 50 μm. Surface ζ potential of calcined powders in water was negative. With the increase of calcination temperature, ζ potential increased gradually. The larger the ζ potential was, the better the adsorption capability would be. The adsorption capability to cationic dyes was stronger than anionic dyes. For crystal violet, methylene blue, and rhodamine B, the best adsorption capability was 33.96, 10.08, and 2.04 mg/g, respectively. In addition, the greater the solubility parameter of the dye molecule was, the less the amount of dye to be adsorbed. A fine trend was observed between solubility parameter and adsorption capability.

Keywords: Blueberry pomace; Diatomite; Calcination; Adsorption; Dye wastewater

1. Introduction

The textile industry plays a significant role in China's economy, but it produces abundant dye wastewater with high concentration. Dye wastewater is a source of industrial pollutants, causing serious threat to water ecosystems. According to reports, due to unimproved treatment technology, 10%–20% colorants are drained from wastewater in the dye industry [1,2]. Massive wastewater without effective treatment that flows into rivers and lakes will cause serious pollution to water. Moreover, the wastewater may contain organisms that can make water systems poisonous and chromatic. Wastewater will also reduce the amount of sunlight into water and decrease photosynthesis [3]. Thus, this kind of dye wastewater should be treated. At present, many methods have been used in treating dye wastewater, which can generally be divided into physicochemical,

chemical and biochemical processes [4–6]. The functions and effects of these methods are different. Nonetheless, all of them have some certain effects on treating dye wastewater. Adsorption is one of the most applied physicochemical methods. In recent years, the study of utilizing cheap adsorption materials, such as zeolite, fly ash, sawdust, slag, and mineral clay among others, to replace the traditional activated carbon to treat dye wastewater has attracted worldwide attention [7]. In China, diatomite is a rich and cheap nature resource, which is expected to be an ideal adsorbent because of its porous structure [8–12].

In recent years, with the bloom of blueberry industries worldwide, the form of blueberry products is becoming more and more various. Juice products occupy substantial proportion among the blueberry products. In the production and processing of blueberry juice, diatomite is usually used as filter aid [13–17]. Thus, the waste blend of diatomite and blueberry pomace is produced. With the increase of juice processing output, a large amount of blueberry pom-

---

*Corresponding author.

ace containing diatomite also appeared. Fruit residue after juicing still contains many organic matters, with high moisture content. If exposed in wet air, the residue is oxidized, thus generating putrefactive odor and polluting the environment. Therefore, the exploration of reusing the waste blueberry pomace is a significant work [18].

Although few anthocyanins are found in the blueberry pomace, the extraction of the anthocyanin residue is difficult [19]. Calcination is a simple and cheap method; hence, the preparation of adsorption material through calcining the waste diatomite containing blueberry pomace will be a promising way for the treatment of dye wastewater. In this study, the high-temperature calcination method was applied to treat the waste diatomite containing blueberry pomace at 500, 550, 600, 650, and 700°C. The adsorption capability of the calcined products for adsorbing five dyes, namely, crystal violet, methylene blue, rhodamine B, eosin Y, and methyl orange was explored. Infrared spectroscope, X-ray diffractometer, laser particle analyzer, and scanning electron microscope were used to characterize the calcined products. The adsorption results were discussed with the surface acidic property, ζ potential, solubility parameter theory, and molecular structure of the dyes.

2. Materials and methods

2.1. Materials

Crystal violet, methylene blue, rhodamine B, eosin Y, methyl orange were purchased from Leheng Science and Technology Co,. Ltd (Shenyang, China). Natural diatomite was produced by Linjiang Changbai Mountain Filter Aid Co,. Ltd (Linjiang, China). The waste diatomite was obtained from a blend composed of fresh blueberry and diatomite with the mass ratio of 10: 1. The blend was used to make a kind of blueberry juice in our laboratory.

2.2. Preparation of calcined product

50 g of the waste diatomite was placed in a crucible. The beginning temperature in muffle furnace was 100°C. Five final calcination temperatures were chosen as 500, 550, 600, 650 and 700°C, respectively. The temperature increasing rate was about 15°C/min.

2.3. Characterization of calcined product

The infrared spectrometer of the calcined products was measured with a Spectrum 400 type Fourier transform mid infrared-near infrared spectrometer (American PE Company, USA). XRD analyses were performed on a D/Max2200 diffractometer (Rigaku, Japan) with a Cu Kα radiation at 40 kV and 30 mV. The scanning step distance was 0.02°. The surface morphology of the calcined products was observed by JSM–7500F SEM of Japan Electronics Corporation.

The particle size and specific surface area of the calcined products were determined by Master sizer 2000 laser particle sizer (Malvern, UK). The sample was first soaked with a small amount of 0.5% of $(NaPO_3)_6$ solution. Then the solution was dispersed under sonication. When

the sample was dispersed sufficiently, measurement was carried out.

2.4. Measurement of adsorption capability of calcined product

The measurement was performed at room temperature. The five dyes were prepared into a 10 mg/L solution. 0.50 g calcined powder was packed into an adsorption column with a volume of 20 mL. After wetting the packed powder with a small amount of ethanol, the dye solution was fed into the column with a peristaltic pump. When the solution flowed through the packed powder, dye molecules were adsorbed by the powder. For different dyes, the entire adsorption process lasted about 3–7 h.

The adsorption capability Q (mg/g) of the calcined powder to dye is defined as the mass of adsorbed dye by one gram of the calcined powder as follows:

$$Q = 2\sum_{C_f=0}^{C_f=8}(10 - C_f)V_{C_f} \tag{1}$$

where C_f (mg/L) is the concentration of the filtrated solution and V_{Cf} (mL) is the total volume of filtrated solution with a concentration lower than C_f (mg/L). The concentration of the filtrated solution was measured with a UV-vis spectrometer (T6 new century, China).

2.5. Measurement of ζ potential of calcined product

ζ potential is an important parameter used to describe the surface characteristic of solid particles. The ζ potential of the calcined powder was measured by streaming potentiometry method on a self-made device. KCl solution with a concentration of 0.01 mol/L was taken as the media. The equation for the calculation of ζ potential is as follows [20].

$$\zeta = \frac{4\pi\mu\kappa}{\varepsilon_0\varepsilon_r} \cdot \frac{\Delta E}{\Delta P} \tag{2}$$

where ζ is the zeta potential (mV), ΔP is the pressure difference (Pa), ΔE is the streaming potential (mV), μ is the viscosity coefficient of KCl solution (Pa·s), κ is the conductivity of KCl solution (S·m⁻¹), ε_0 is the absolute permittivity of vacuum (F·m⁻¹), and ε_r is the relative permittivity of KCl solution.

3. Results and discussion

3.1. Infrared spectrum analysis of calcined product

Diatomite is a kind of biogenic siliceous sedimentary rocks. Its chemical composition is mainly SiO_2. The impurity includes Fe_2O_3 and Al_2O_3, to name a few [21]. The mineral composition of diatomite is mainly opal ($SiO_2·H_2O$, also called amorphous silica). The associated mineralsare kaolinite, illite, and montmorillonite, among others. The infrared spectra of the samples calcined at different temperatures are shown in Fig. 1. As shown in Fig. 1, the peak at 1635 cm⁻¹ is the flexural vibration adsorption peak of water molecule and 3426 cm⁻¹ is the stretching vibration peak of hydroxyl of water molecule [22]. Three strong adsorption peaks appear at 462, 798, and 1098 cm⁻¹ which belong to the vibration
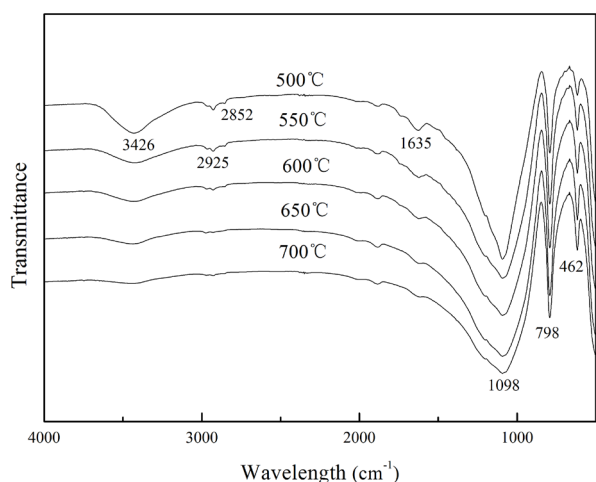
Fig. 1. FT-IR spectra of waste diatomite calcinated at different temperatures.

peaks of Si–O groups in opal [23,24]. This finding means that the main phase of the calcined products is amorphous opal. The peaks at 2852 and 2925 cm^{-1} belong to the long alkyl groups of the residue organic matter in the calcined products [25]. When the calcination temperature is above 600°C, the strength of the characteristic peaks of organic matter decreases until the peaks disappear.

3.2. X-ray diffraction pattern analysis of calcined product

The XRD spectra of different calcined products are shown in Fig. 2. The position of the main diffraction peak of the diatomite is the same as reported in the literature [26]. The diffraction peaks of quartz and anorthite appear at 500°C. When the calcination temperature reached 700°C, the position of the main diffraction peaks does not change, which means that no obvious change is observed in the silica phase and the structure of diatom shell was not destroyed.
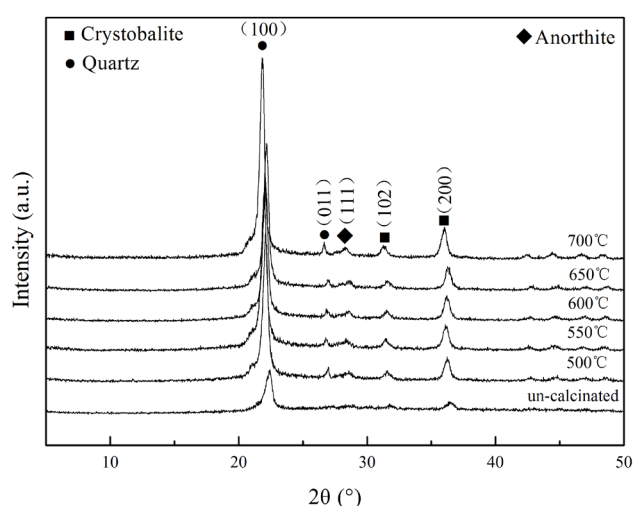

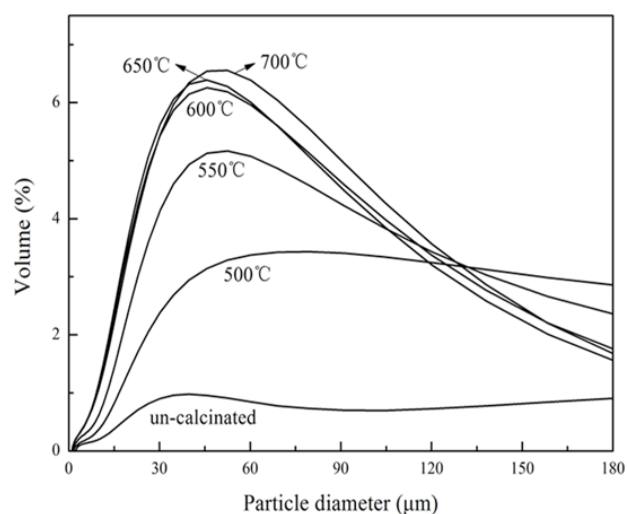Fig. 2. XRD patterns of waste diatomite calcinated at different temperatures.

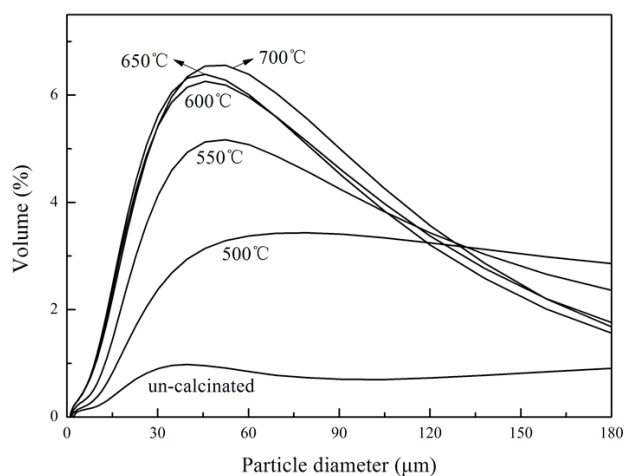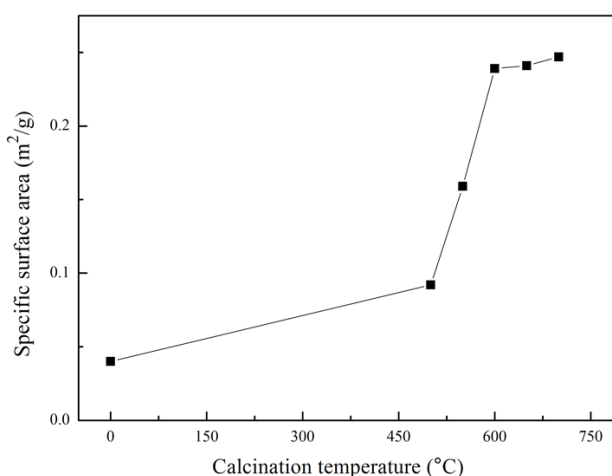Fig. 4. Specific surface area of waste diatomite calcinated at different temperatures.

Fig. 3. Particle size distribution of waste diatomite calcinated at different temperatures.

3.3. Particle size and specific surface area of calcined product

The particle size distribution of different calcined products is shown in Fig. 3. The average particle diameter of the calcined powders was between 40 μm and 50 μm. When the calcination temperature was increased from 500°C to 700°C, the average particle diameter slightly decreased because the coarse particles were destroyed by thermal decomposition under high temperature. The specific surface area of different calcined products is shown in Fig. 4. As shown in Fig. 4, the specific surface area increases with the rise of the temperature. Blended organic matter was decomposed at high temperature; hence, more pores would form in the calcined powder.

3.4. Morphology analysis of calcined products

The SEM photographs of un-calcinated sample, including two products calcined at 500°C and 700°C are shown in Fig. 5. As shown in the figure, no obvious morphology change is observed for the three samples. When the calcination temperature reached 700°C, the shape of the disk shell is still clear and complete. This finding also means that the diatom shell did not melt.

3.5. Adsorption capability of calcined product to five dyes

Fig. 6 shows the plots of the adsorption capability of waste diatomite versus the calcination temperature. As shown in Fig. 6a, with the increase of calcination temperature, the adsorption capability of calcined products to the three dyes decreased gradually. The adsorption capability of calcined products to crystal violet was greater than that of methylene blue, and the adsorption capability of the calcined products to rhodamine B was the weakest. Fig. 6b shows the adsorption capability to eosin Y and methyl orange. As shown in Fig. 6b, the adsorption capability of the calcined products to eosin Y and methyl orange was best at a calcination temperature of 600°C and 650°C, respectively. The adsorption capability of the calcined products to eosin Y was greater than that of methyl orange. However, compared with Fig. 6a, the adsorption capability of the calcined products to both was poor.

According to the study of Yuan et al., there were no acid sites in the un-calcinated diatomite [27]. After calcination, acid sites would appear at the surface of the calcinated diatomite and the maximum quantity of acid sites would reach at 650°C [27]. In this work, the five dyes can be divided into two categories according to the charge type of
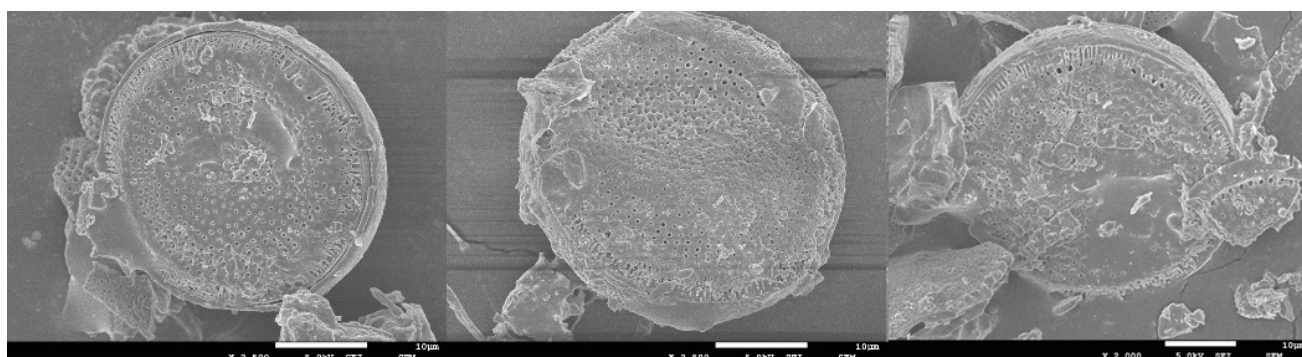

Fig. 5. SEM images of waste diatomite calcinated at different temperatures. (a) un-calcinated, (b) 500°C, (c) 700°C.
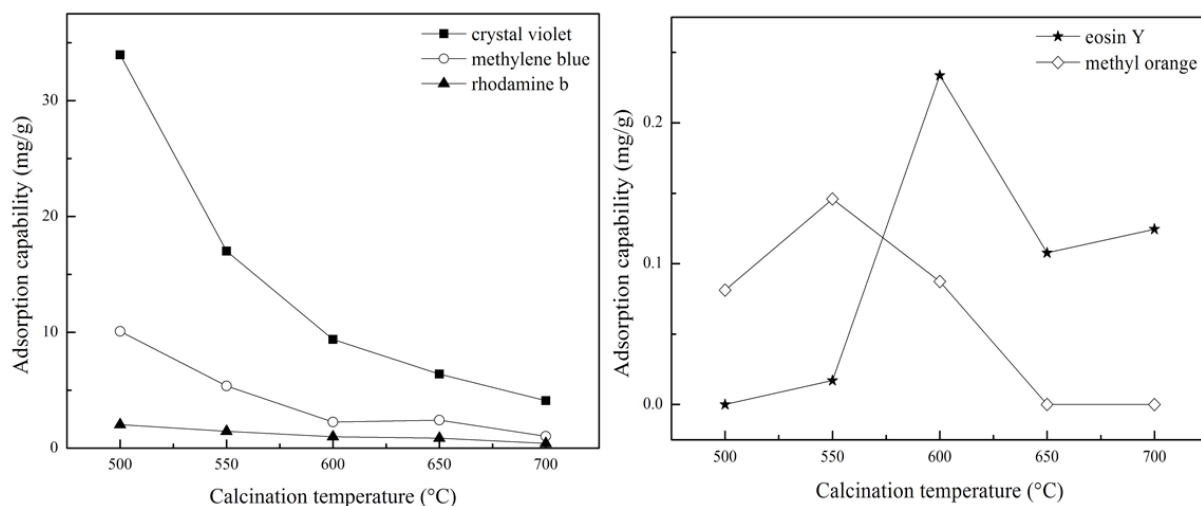

Fig. 6. Adsorption capability of waste diatomite calcinated at different temperatures. (a) crystal violet, methylene blue, rhodamine B. (b) eosin Y, methyl orange.
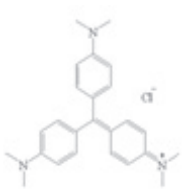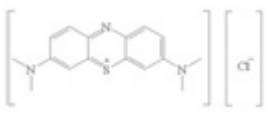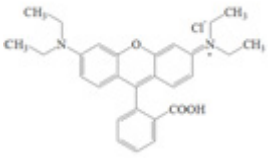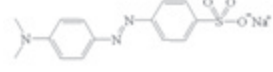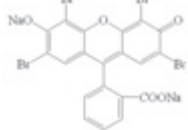
their main body as shown in Table 1. Crystal violet, methylene blue, and rhodamine B are the cationic dyes. Eosin Y and methyl orange are the anionic dyes.

The acid sites will repel the dyes with positive charge. Therefore, for the three dyes of crystal violet, methylene blue and rhodamine B, their adsorption capability decreased with the increase of calcination temperature due to the quantity of acid sites of the calcinated diatomite increased with the calcination temperature.

3.6. ζ potential of calcined product

The ζ potential of the calcined products at different calcination temperatures was calculated by Eq. (2), and the results are shown in Fig. 7. As shown in Fig. 7, with the increase of the calcination temperature, the ζ potential increased gradually. The increase trend of ζ potential versus calcination temperature is also in agreement with the increasing acid sites as found by Yuan et al. [27]. Considering the effects of crystal violet, methylene blue and rhodamine B ionized to cationic ions in solution, and the surface of the calcined powder was electronegative, the calcined powder was apt to adsorb the cationic dyes, such as crystal violet, methylene blue, and rhodamine B (as shown in Fig. 6).

The comparison of adsorption capabilities with other seven adsorbents reported in literatures are listed in Table 2. It shows that for adsorbing methylene blue and crystal violet, the adsorption capabilities of the calcined waste diatomite prepared in this work are stronger than the other adsorbents.

3.7. Relationship between adsorption capability and Hansen solubility parameter of dyes

Solubility parameter δ is a physical constant, which can be used to estimate the interaction strength between two phases. It is defined as the square of cohesive energy density. The total solubility parameter δ includes three parts:

$$\delta^2 = \delta_d^{\,2} + \delta_p^{\,2} + \delta_h^{\,2} \tag{3}$$

where δ_d, δ_p, and δ_h are the dispersion solubility parameter, polar solubility parameter, and hydrogen bonding solubility parameter, respectively. The solubility parameters of the five dyes could be calculated from the data listed in Hansen's handbook [33] and are listed in Table 3.
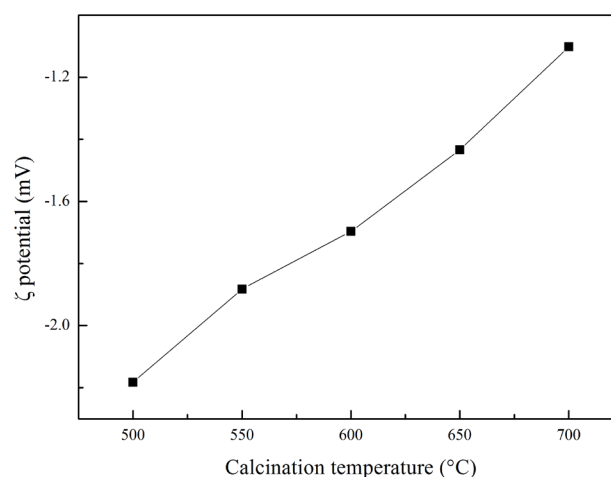

Fig. 7. ζ potential of waste diatomite calcinated at different temperatures.

Table 1
Classification of five dyes

Name	Structure	Classification according to the electric charge of main body
Crystal violet		Cationic dye
Methylene blue		Cationic dye
Rhodamine B		Cationic dye
Methyl orange		Anionic dye
Eosin Y		Anionic dye

Table 2
Comparison of adsorption results with other literatures

Adsorbent	Dye	
	Methylene blue	Crystal violet
Ultra-fine fly ash based adsorbent [28]	0.83 mg/g	–
Supersiliceous zeolite ZSM-5 [29]	6.08 mg/g	–
Halloysite nanotubes modified with silane coupling agent [30]	8.91 mg/g	–
Banana peel powder [31]	–	11.79 mg/g
Kaolin modified with iron salt [32]	–	17.32 mg/g
Diatomite/nano titanium silicalite [33]	–	20.13 mg/g
Camellia oleifera shell [34]	–	26.93 mg/g
Calcined waste diatomite in this work	10.08 mg/g	33.96 mg/g

Table 3
Solubility parameters of five dyes

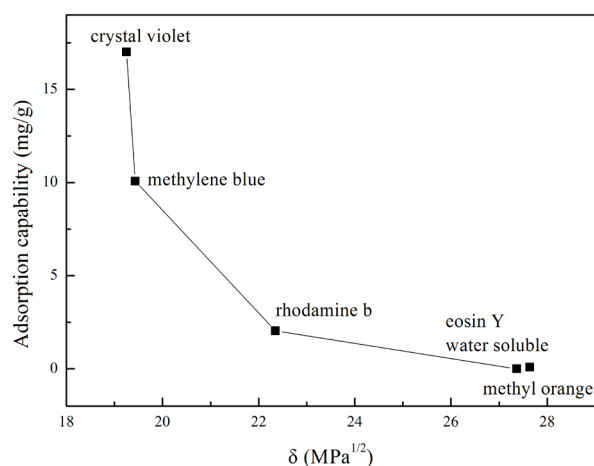| Name	δ_d (MPa$^{1/2}$)	δ_p (MPa$^{1/2}$)	δ_h (MPa$^{1/2}$)	δ (MPa$^{1/2}$)
Crystal violet	19.07	1.72	1.98	19.25
Methylene blue	19.26	1.66	1.91	19.43
Rhodamine B	21.22	4.00	5.76	22.35
Eosin Y	24.49	8.52	8.77	27.37
Methyl orange	17.72	14.65	15.34	27.64

Fig. 8. Plot of adsorption capability versus total solubility parameters of five dyes for the powder calcined at 500°C.

Fig. 8 shows the plot of adsorption capability versus the total solubility parameters of five dyes for the powder calcined at 500°C. As shown in Fig. 8, the greater the solubility parameter of the dye molecule was, the less the amount of dye to be adsorbed. A fine trend is observed between the solubility parameter and adsorption capability for the five dyes.

4. Conclusion

When the calcination temperature was above 600°C, the organic matter in the waste diatomite would be decomposed thoroughly. For the waste diatomite calcined between 500°C and 700°C, no obvious change was observed in the silica phase and the structure of diatom shell was not destroyed. The average particle diameter of the calcined products was between 40 μm and 50 μm. When the calcination temperature was increased from 500°C to 700°C, the average particle diameter of the calcined products slightly decreased and the specific surface area was increased. The surface ζ potential of the calcined powders in water was negative. With the increase of the calcination temperature, the ζ potential increased gradually. The larger the ζ potential was, the better the adsorption capability of the calcined products to the dyes would be. Crystal violet, methylene blue, and rhodamine B were the cationic dyes. Eosin Y and methyl orange were the

anionic dyes. The adsorption capability of the calcined products to the cationic dyes was stronger than that of the anionic dyes. The best adsorption capability of the calcined product was obtained at 500°C. For crystal violet, methylene blue, and rhodamine B, the best adsorption capability was 33.96, 10.08, and 2.04 mg/g, respectively. In addition, the greater the solubility parameter of the dye molecule was, the less the amount of dye to be adsorbed. A fine trend was observed between solubility parameter and adsorption capability for the five dyes.

Acknowledgement

References

[1] M.V. Sureshkumar, C. Namasivayam, Adsorption behavior of Direct Red 12B and Rhodamine B from water onto surfactant-modified coconut coir pith, Colloids Surf., A, 317(1–3) (2008) 277–283.

[2] J. Skubiszewska-Zięba, B. Charmas, R. Leboda, V.M. Gun'ko, Carbon-mineral adsorbents with a diatomaceous earth/perlite matrix modified by carbon deposits, Microporous Mesoporous Mater., 156(18) (2012) 209–216.

[3] D. Karadag, M. Turan, E. Akgul, S. Tok, A. Faki, Adsorption equilibrium and kinetics of Reactive Black 5 and Reactive Red 239 in aqueous solution onto surfactant-modified zeolite, J. Chem. Eng. Data, 52(5) (2007) 1615–1620.

[4] A.B.D. Santos, F.J. Cervantes, J.B.V. Lier, Review paper on current technologies for decolourisation of textile wastewaters: perspectives for anaerobic biotechnology, Bioresour. Technol., 98(12) (2007) 2369–2385.

[5] E. Forgacs, T. Cserhati, G. Oros, Removal of synthetic dyes from wastewaters: a review, Environ. Int., 30 (2004) 953–971.

[6] T. Robinson, G. McMullan, R. Marchant, P. Nigam, Remediation of dyes in textile effluent: a critical review on current treatment technologies with a proposed alternative, Bioresour. Technol., 77 (2001) 247–255.

[7] M. Šljivić, I. Smičiklas, S. Pejanović, I. Plećaš, Comparative study of Cu^{2+} adsorption on a zeolite, a clay and a diatomite from Serbia, Appl. Clay Sci., 43(1) (2009) 33–40.

[8] Z. Al-Qodah, W.K. Lafi, Z. Al-Anber, M. Al-Shannag, A. Harahsheh, Adsorption of methylene blue by acid and heat treated diatomaceous silica, Desalination, 217(1) (2007) 212–224.

[9] B. Gao, P. Jiang, F. An, S. Zhao, Z. Ge, Studies on the surface modification of diatomite with polyethyleneimine and trapping effect of the modified diatomite for phenol, Appl. Surf. Sci., 250(1–4) (2005) 273–279.

[10] J.L. Wu, Y.S. Yang, J.H. Lin, Advanced tertiary treatment of municipal wastewater using raw and modified diatomite, J. Hazard. Mater., 127(1–3) (2005) 196.

[11] Y. Aldegs, M.A. Khraisheh, M.F. Tutunji, Sorption of lead ions on diatomite and manganese oxides modified diatomite, Water Res., 35(15) (2001) 3724.

[12] M.A. Al-Ghouti, M.A.M. Khraisheh, M. Tutuji, Flow injection potentiometric stripping analysis for study of adsorption of heavy metal ions onto modified diatomite, Chem. Eng. J., 104(1–3) (2004) 83–91.

[13] N. Ediz, B. İsmail, T. İlknur, Improvement in filtration characteristics of diatomite by calcination, Int. J. Miner. Process., 94(3–4) (2010) 129–134.

[14] J. Gómez, M.L. Gil, I.R.N. De, M. Alguacil, Diatomite releases silica during spirit filtration, Food Chem., 159(159) (2014) 381–387.

[15] D.D.N. Af, G.A. EI, S. Frangie, V. Martinez, L. Valiente, O.A. Webb, Turning the volume down on heavy metals using tuned diatomite. A review of diatomite and modified diatomite for the extraction of heavy metals from water, J. Hazard. Mater., 241–242(4) (2012) 14.

[16] H. Yu, B. Fugetsu, A novel adsorbent obtained by inserting carbon nanotubes into cavities of diatomite and applications for organic dye elimination from contaminated water, J. Hazard. Mater., 177(1–3) (2010) 138.

[17] C.D. Wu, X.J. Xu, J.L. Liang, Q. Wang, Q. Dong, W.L. Liang, Enhanced coagulation for treating slightly polluted algae-containing surface water combining polyaluminum chloride (PAC) with diatomite, Desalination, 279(1) (2011) 140–145.

[18] J. Lee, R.W. Durst, R.E. Wrolstad, Impact of juice processing on blueberry anthocyanins and polyphenolics: comparison of two pretreatments, J. Food Sci., 67(5) (2010) 1660–1667.

[19] G. Skrede, R.E. Wrolstad, R.W. Durst, Changes in anthocyanins and polyphenolics during juice processing of highbush blueberries (Vaccinium corymbosum L.), J. Food Sci., 65(2) (2000) 357–364.

[20] H. Hu, A. Yu, E. Kim, B. Zhao, M.E. Itkis, A.E. Bekyarova, Influence of the zeta potential on the dispersability and purification of single-walled carbon nanotubes, J. Phys. Chem. B, 109(23) (2005) 11520–11524.

[21] W. Liu, Modeling description and spectroscopic evidence of surface acid-base properties of natural illites, Water Res., 35(17) (2001) 4111–4125.

[22] M.A.M. Khraisheh, M.S. Alg-Houti, Enhanced dye adsorption by microemulsion-modified calcined diatomite (μE-CD), Adsorption, 11(5) (2005) 547–559.

[23] W.S. Xiao, W.S. Peng, G.X. Wang, F.Y. Wang, K.N. Weng, Infrared spectroscopic study of Changbaishan diatomite, Spectrosc. Spectral Anal. (Beijing, China), 24(6) (2004) 690–693.

[24] H.L. Wang, L.I. Jin-Hong, L. Hou, F. Liu, M.A. Xi, Study on the pozzolanic activity of diatomite, Bull. Chin. Ceram. Soc., 30(1) (2011) 18–19.

[25] R.A. Shawabkeh, M.F. Tutunji, Experimental study and modeling of basic dye sorption by diatomaceous clay, Appl. Clay Sci., 24(1–2) (2003) 111–120.

[26] P. Yuan, D. Liu, M.D. Fan, D. Yang, R.L. Zhu, F. Ge, Removal of hexavalent chromium [Cr(VI)] from aqueous solutions by the diatomite-supported/unsupported magnetite nanoparticles, J. Hazard. Mater., 173(1–3) (2010) 614.

[27] P. Yuan, D.Q. Wu, H.P. He, Z.Y. Lin, The hydroxyl species and acid sites on diatomite surface: a combined IR and Raman study, Appl. Surf. Sci., 227(1) (2004) 30–39.

[28] Y.J. Zhao, X.C. Zhao, Y.R. Jiang, Kinetics of adsorption of methylene blue from aqueous solution by ultra-fine fly ash based adsorbents, J. Xi'an Univ. of Arch. & Tech., 22(7) (2009) 133–135.

[29] X. Jin, M.Q. Jiang, X.Q. Shan, Z.G. Pei, Z. Chen, Adsorption of methylene blue and orange II onto unmodified and surfactant-modified zeolite, J. Colloid Interface Sci., 328(2) (2008) 243.

[30] L.F. Cai, B.Y. Zheng, F.U. Ming-Lian, L.F. Cai, Modification of halloysite nanotubes and their adsorption on methylene blue, J. Putian Univ., (2012).

[31] H. Fang, R. Zhang, P. Lv, R. Li, B. Zhou, L. Zhang, Adsorption kinetics and thermodynamics of banana peel powder on crystal violet wastewater, New Chem. Mater., (2014).

[32] X.Y. Jin, W.R. Chen, M. Zheng, H.H. Lai, Z.L. Chen, A study on adsorption performance of crystal violet from the wastewater modified kaolin, Acta Mineral. Sin., 32(2) (2012) 254–258.

[33] W.W. Yuan, Investigation on the preparation of diatomite-based porous mineral materials and their adsorption/catalysis performance on the organic pollutants, Guangzhou Institute of Geochemistry, Chinese Academy of Sciences, 2016.

[34] D. Song, H. Guo, L. Yan, Adsorptive property of crystal violet on camellia oleifera shell in aqueous solution, Chin. J. Environ. Eng., 8(12) (2014) 5129–5134.

[35] C.M. Hansen, Hansen Solubility Parameters: A User's Handbook, CRC Press, 2013.